npj | climate and atmospheric science

Article

Published in partnership with CECCR at King Abdulaziz University

https://doi.org/10.1038/s41612-026-01403-x

Large direct and indirect impacts of ozone-depleting substances on past Southern Hemisphere atmosphere-ocean trends

Check for updates

Michael Sigmond[1] ✉ & Lorenzo M. Polvani[2,3]

The indirect impacts of ozone-depleting substances (ODSs) on past Southern Hemisphere (SH) climate change via their impact on the ozone layer have been widely documented, but their direct radiative impacts remain unexplored. Using 20-member ensembles of historical simulations with a state-of-the-art climate model, we quantify this direct impact and compare it with their indirect impact via ozone depletion, as well as with the impacts of tropospheric ozone, CO_2 and aerosols. We find that the radiative impacts of ODSs contributed substantially to annual-mean SH atmosphere and ocean circulation trends between 1955 and 2000, with impacts nearly as large as those of stratospheric ozone, and exceeding those of CO_2. ODSs also account for 29% of Southern Ocean warming, several times the individual contributions from stratospheric and tropospheric ozone. Our findings highlight the major role of ODSs in SH climate change and underscore the importance of the Montreal Protocol in mitigating climate change.

The rapid increase in ozone-depleting substances (ODSs) after the 1950s resulted in the severe depletion of stratospheric ozone in the late 20th century. Following the discovery of the ozone hole over Antarctica[1], the international community agreed to phase out ODSs under the 1987 Montreal Protocol and its subsequent amendments. This has not only resulted in the onset of the recovery of the stratospheric ozone layer[2], but has also prevented substantial global warming[3] since ODSs are also potent greenhouse gases[4]. Climate modeling experiments are needed to separately quantify both the direct (i.e., radiative) and indirect (i.e., ozone-depletion-mediated) impacts of ODSs on the climate system. Unfortunately, such experiments are not routinely performed within internationally coordinated model intercomparison projects, where simulations routinely combine all GHGs (including ODSs) into a single forcing, making it impossible to separate the impacts of ODSs from other GHGs such as carbon dioxide (CO_2). These simulations also typically lump together stratospheric and tropospheric ozone into a single forcing[5,6], despite the fact that the sources of these gases are totally different.

In recent years, a few groups have started to run bespoke climate modeling experiments to quantify the climate impacts of substances regulated under the Montreal Protocol. These experiments have identified a large impact of the radiative effects of ODSs on global and Arctic climate trends during the second half of the 20th century[7–10]. In particular, ref. 9 (hereafter S23) showed that ODSs collectively represented the second largest contributor to climate warming after CO_2, accounting for roughly one third of total human-induced global warming, Arctic warming and Arctic sea ice loss. However, detailed studies of the radiative impacts of ODSs on the Southern Hemisphere (SH) atmosphere-ocean climate are currently lacking.

By contrast, a large body of literature has established that stratospheric ozone depletion (the result of increasing concentrations of ODSs) has been the main driver of the significant trends in SH atmospheric circulation that have been observed in the second half of the 20th century[11–19]. These changes include a poleward shift and intensification of the SH jet stream, accompanied with regional patterns in surface temperature trends and a poleward shift of precipitation patterns[19–21]. In the annual mean, GHGs have been shown to play a substantial role as well[14], but the separate contribution of ODSs to the GHG-driven circulation trends is yet to be quantified.

Attributing these atmospheric circulation trends is important not only for interpreting regional surface temperature and precipitation trends, but also for understanding past trends in sea surface temperatures (SSTs) and

[1]Canadian Centre for Climate Modelling and Analysis, Environment and Climate Change Canada, Victoria, BC, Canada. [2]Department of Applied Physics and Applied Mathematics, Columbia University, New York, NY, USA. [3]Lamont Doherty Earth Observatory, Columbia University, Palisades, NY, USA.
✉e-mail: Michael.Sigmond@ec.gc.ca

ocean circulation. For example, trends in surface wind stress driven by stratospheric ozone depletion have been shown to contribute to a tripole pattern in SST trends through their impacts on sensible heat fluxes, Ekman transport and mixed layer depth[22–24], and to induce changes in the ocean meridional overturning circulation[14,25–27]. Such trends may have had global implications through their impact on the ocean carbon sink[27–30].

Previous studies have identified increasing GHGs as the main driver of the rapid Southern Ocean warming observed over the second half of the 20th century[31–33], but the specific contribution of ODSs to this GHG induced warming remains unclear. Two recent studies have attempted to separate the oceanic impacts of the gases relevant to the Montreal Protocol from the impacts of other GHGs, but neither performed a fully satisfactory decomposition. One study[33] formally detected in the past Southern Ocean warming, the separate fingerprints of all GHGs combined (including ODSs) and of stratospheric ozone. It found that stratospheric ozone depletion played a quantitatively minor role compared to GHGs; however, it did not separately quantify the individual contribution of ODSs and of CO_2. A second study[26] isolated the impact on the SH ocean resulting from "the formation of the ozone hole". Using a chemistry-climate model, it found that the formation of the ozone hole accounted for approximately 30% of 20th century Southern Ocean warming; however, it was unable to separately quantify the direct radiative impacts from ODSs from the accompanying depletion of stratospheric ozone (such a decomposition cannot be done easily when ozone is interactively computed in the model).

In this study, we provide the first comprehensive assessment of both the direct radiative impacts of ODSs and their indirect impacts through stratospheric depletion on SH atmosphere and ocean trends. In addition, we quantitatively compare those impacts to those of increasing CO_2 (the largest contributor to climate change) and tropospheric ozone (as a recent study found its trends contributed more to Southern Ocean warming than stratospheric ozone trends[34]). To this end, we analyze five 20-member ensembles of historical simulations conducted with version 5 of the Canadian Earth System Model (CanESM5)[35]. In each ensemble, one forcing agent—ODSs, CO_2, stratospheric ozone, tropospheric ozone, or aerosols—is held fixed at 1955 levels, while all other forcings follow their observed historical evolution. The climate impact of each agent is diagnosed as the difference relative to the standard historical simulations in which all forcings follow their observed historical evolution. The climate response to individual agents is quantified as the linear trend over the 1955–2000 period multiplied by 45 (see Methods), averaged over each ensemble. We emphasize that one cannot naively examine the entire period from 1955 to the present period with a single linear trend, as both stratospheric ozone and ODS concentrations are *not* linear functions of time: owing to the implementation of the Montreal protocol in the 1990s, their concentrations have plateaued in the early 21st century. It has become customary, therefore, to separate the pre- and post–2000 periods, to which individual linear trends can be applied[36–38] Since we wish to bring out the largest contribution from ODSs and stratospheric ozone, we here focus on the 1955–2000 period, when their concentrations show the largest trends (see Supplementary Fig. 1). We note that our model does not include interactive chemistry, and thus the ozone field is simply prescribed using the standard CMIP6 ozone dataset. A caveat of this approach is that a fully interactive ozone simulation may be required to fully capture the ozone impacts on the climate[39]. On the other hand, this approach has a critical advantage in that it allows us to separate the direct radiative effect of ODS from their indirect effect via ozone depletion. We will show that the direct effects of ODSs have made a surprisingly large contribution to late 20th century SH atmosphere and ocean trends.

Results

Atmosphere

We begin by examining historical trends in the latitudinal position of the SH midlatitude jet. We first note that the historical simulations with CanESM5 (Fig. 1, gray bars) successfully capture the observed poleward shift of the SH jet between 1955 and 2000, both in austral summer (Fig. 1a) and in the annual mean (Fig. 1b). In both cases, the model ensemble spread (gray error bars) encompasses the observation-based estimate (green dots), providing strong evidence that the model is suitable for quantifying the contributions of individual forcings to SH jet position trends over this period. Consistent with the literature described in the introduction, we find that in the austral summer, stratospheric ozone is the main driver of the SH jet trends, accounting for roughly half of the 1955–2000 shift. In fact, none of the other forcings considered here, including carbon dioxide, produce a statistically significant response in austral summer over the period of interest.

However, this picture changes when considering the annual mean (Fig. 1b). Here, we do find a significant response to stratospheric ozone, as expected, but also a surprisingly large direct (i.e., non-ozone-mediated) response to ODSs. A first key result of this study, therefore, is that in the annual mean the direct radiative ODS contribution to SH jet trends is substantial—only slightly smaller than the one from stratospheric ozone depletion, and larger than the contribution from CO_2. Given that the global mean temperature response to ODSs is only ~60% of that due to CO_2 (S23), this implies that, per degree of global warming, ODSs were considerably more effective than CO_2 at shifting the SH jet.

To provide a fuller picture of the zonal wind response, Fig. 2 shows the contribution of the individual forcings to the vertical structure of the zonal-mean zonal wind changes over the 1955–2000 period. We note that the observed changes are similar to those in the historical (i.e., all forcing) CanESM5 simulations (Supplementary Fig. 2, keeping in mind that the observed changes are a single realization, and thus are not expected to exactly match the ensemble mean changes). As in the case of the tropospheric jet shift, we find that stratospheric ozone is the largest driver of zonal-mean zonal wind trends throughout the troposphere and stratosphere, not only in austral summer but also in the annual mean. Seasonally, the stratospheric ozone contribution peaks in austral summer (consistent with previous studies), while CO_2 and direct ODS contributions peak in austral fall, when the stratospheric polar vortex is closest to the pole (Supplementary Fig. 3; see also Fig. 3). The bottom row of Fig. 2 shows that in the annual mean, the radiative ODS contribution to both the stratospheric polar vortex and tropospheric zonal wind trends is substantial, again slightly exceeding that of CO_2.

Why do the radiative effects of ODSs exert a stronger influence on the atmospheric circulation than CO_2 despite their smaller contribution to global warming? To address this, we have examined the vertical structure of the temperature responses. CO_2 produces the well-known pattern of stratospheric cooling and tropospheric warming (Supplementary Fig. 4a, e), which, combined with the meridionally sloping tropopause, increases the meridional temperature gradient and strengthens the polar vortex. In contrast, while ODSs produce weaker tropospheric warming (Supplementary Fig. 4f): they also cause a *warming* of the tropical lower stratosphere[40–42], resulting in enhanced meridional temperature gradients in that region. This would explain the stronger jet shift from ODS than from CO_2, as the midlatitude jet in the SH is particularly sensitive to lower-stratospheric temperature gradients[43].

Surface

Moving from zonal winds to surface temperature, Fig. 3 shows the contributions of the individual forcings to SST trends as a function of calendar month and latitude. Consistent with the associated radiative forcing (S23), CO_2 is the largest contributor to 1955–2000 SST warming. Note, however, that the direct response from ODSs is substantial and much larger than the response to either tropospheric or stratospheric ozone. For the latter (Fig. 3c), a latitudinal tripole pattern, previously found[22] with a predecessor version of CanESM5, is clearly seen: it is consistent with the surface wind stress changes (black contours), and has been attributed to changes in wind-driven Ekman transport, sensible heat fluxes and mixed layer depths[23,24]. The SST responses to ODSs, CO_2 and tropospheric ozone also show elements of a tripole pattern, consisting of reduced warming at the latitude with increased winds, peak warming just south of the latitude with reduced winds and reduced warming just north of that, suggesting that these SST patterns are also driven by the overlying wind stress changes.

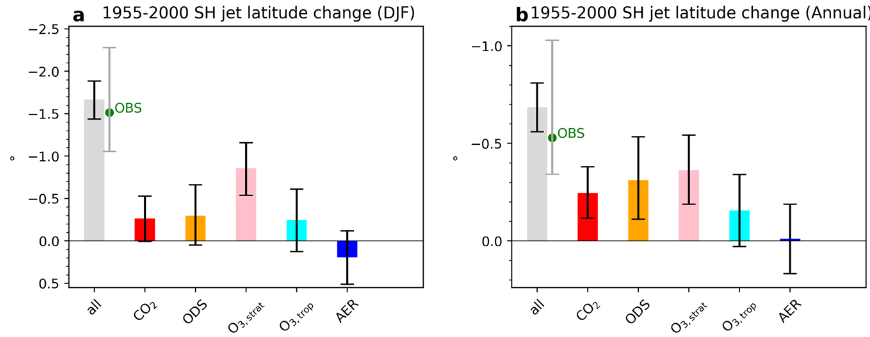

Fig. 1 | SH jet latitude response to individual forcings. **a** December-February (DJF) mean and **b** annual mean SH jet latitude change over the 1955–2000 period due to all historical forcings (all) and CO_2, ODSs, stratospheric ozone ($O_{3,strat}$), tropospheric ozone ($O_{3,trop}$) and aerosols (AER) separately. The black error bars represent the 5–95% confidence range in the ensemble mean (determined by bootstrapping) and the gray error bars the ±1 sigma of the ensemble spread. The green dots denote the observed values from ERA5[54]. The jet latitude is calculated at 500 hPa following the method in ref. 55. Changes are calculated as the linear trend over the 1955–2000 period multiplied by 45.

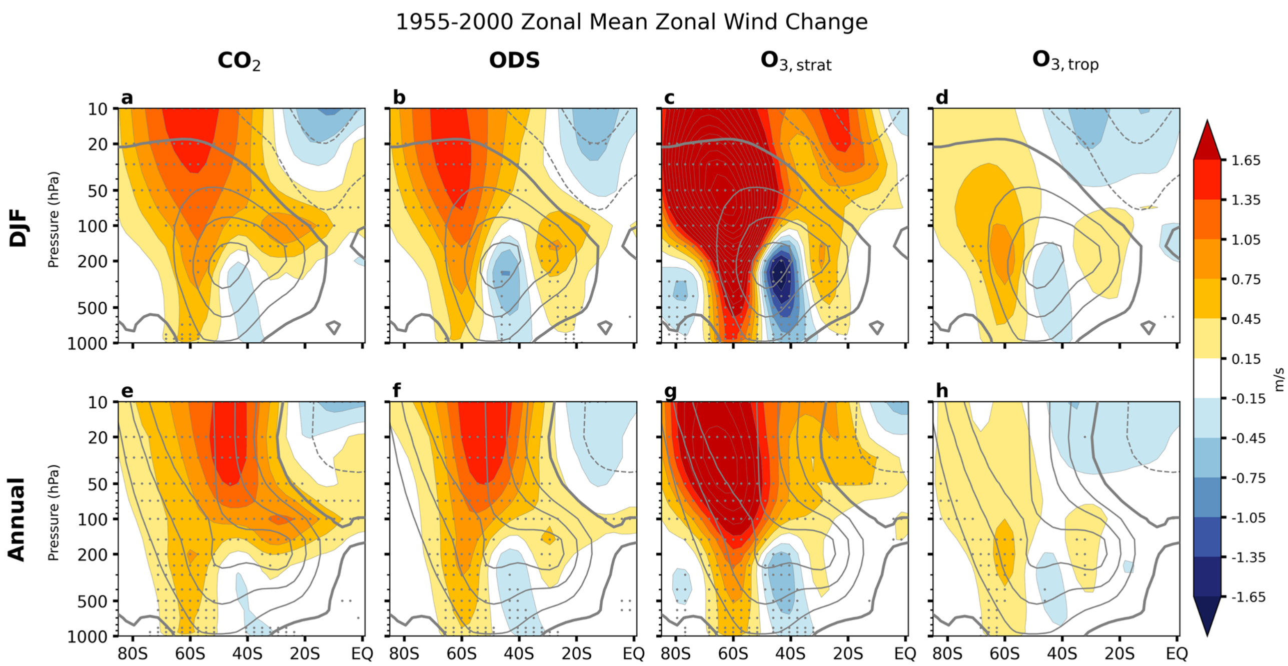

Fig. 2 | Zonal-mean zonal wind response to individual forcings. **a**–**d** December-February (DJF) and **e**–**h** annual mean zonal-mean zonal wind change over the 1955–2000 period due to **a**, **e** CO_2, **b**, **f** ODSs, **c**, **g** stratospheric ozone and **d**, **h** tropospheric ozone. Dots indicate grid points with changes that are statistically significant at the 95% level (determined by bootstrapping). The gray contours represent the climatological zonal-mean zonal wind in all the forcing simulations (contour interval 10 m s^{-1}, with dashed contours representing negative values and the thick line the 0 m s^{-1} contour).

Ocean

Turning now to the vertical structure of ocean temperatures, Fig. 4 shows the zonal mean temperature response to individual forcings as a function of latitude and depth. Again, our model's response resembles the observed trends, with a peak warming just north of the Antarctic Circumpolar Current (ACC) (Supplementary Fig. 5). As in the case of SSTs, Fig. 4 reveals that while CO_2 is the largest driver, the radiative impacts of ODSs have contributed substantially to Southern Ocean warming. The much smaller response to stratospheric ozone is characterized by a tripole pattern, consistent with previous studies[33]. A tripole pattern (superimposed by a uniform warming) is also found in response to the radiative impacts of ODSs and CO_2, consistent with the structure of the peak warming in response to all forcings (Supplementary Fig. 5b).

The black contours in Fig. 4 show the response of the ocean meridional overturning circulation (MOC), which is driven by surface wind stress. Westerly wind stress drives equatorward Ekman transport, convergence and downwelling to the north of the westerly jet and divergence and upwelling to the south[23,44], which is partially compensated by an eddy-driven meridional cell[45,46]. Hence, changes in surface wind stress patterns are expected to drive corresponding changes in the ocean MOC, as seen in Fig. 4. The contribution of stratospheric ozone depletion to ocean MOC changes is the largest (Fig. 4c), consistent with previous studies[14,26]. The novel result here, which constitutes the second major finding, is that the direct radiative impacts of ODSs also play a substantial role in ocean MOC changes and that their contribution is (slightly) larger than that of CO_2, consistent with their larger response to atmospheric circulation changes discussed above. This previously unknown direct impact of ODSs may have had additional global impacts by enhancing the upwelling of natural, carbon-rich waters, thereby reducing the atmosphere-ocean CO_2 partial pressure gradient and weakening the Southern Ocean's capacity to absorb anthropogenic CO_2 emissions[27].

Finally, we shift our attention from the structure of Southern Ocean warming to its total value, as quantified by the Southern Ocean heat content (SOHC). We define SOHC as the heat content integrated over the entire ocean south of 40°S, following ref. 26, but note that qualitatively similar results are found using alternative definitions such as that employed in ref. 34. A comparison of the gray error bar and the green dot in Fig. 5 reveals that CanESM5 successfully captures the observation-based SOHC trends, validating its use for attributing 1955–2000 SOHC changes to individual forcings.

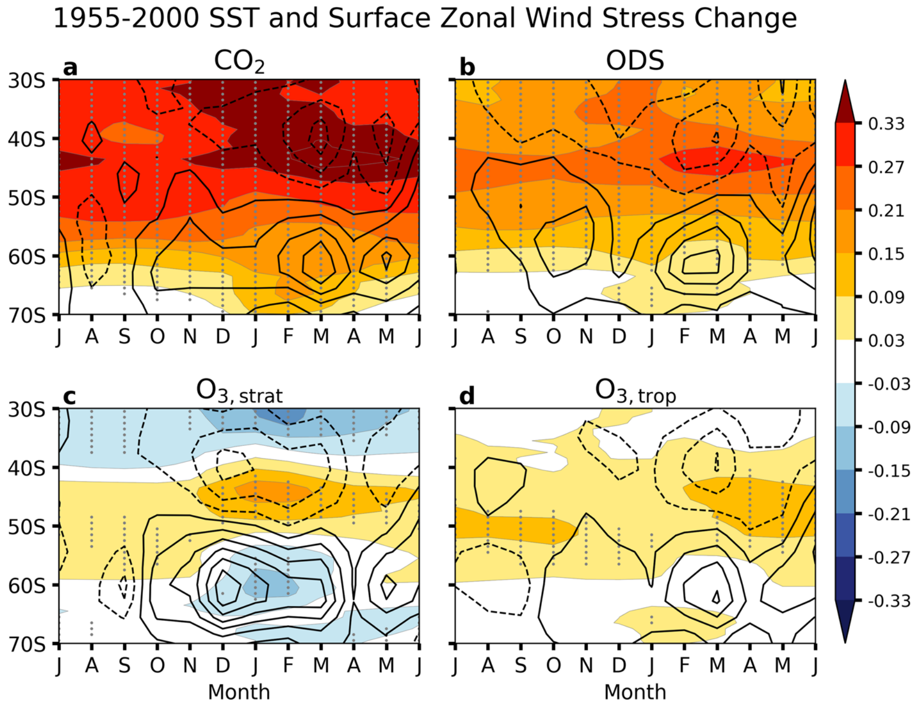

Fig. 3 | Sea Surface Temperature and surface zonal wind stress response to individual forcings. Zonal mean (colors) Sea Surface Temperature (SST) and (contours) surface zonal wind stress wind change over the 1955–2000 period as a function of calendar month and latitude due to **a** CO_2, **b** ODSs, **c** stratospheric ozone, and **d** tropospheric ozone. Dots indicate SST changes that are statistically significant at the 95% level (determined by bootstrapping). The contour interval for surface zonal wind stress is 0.2 m s^{-1}, with dashed contours representing negative values.

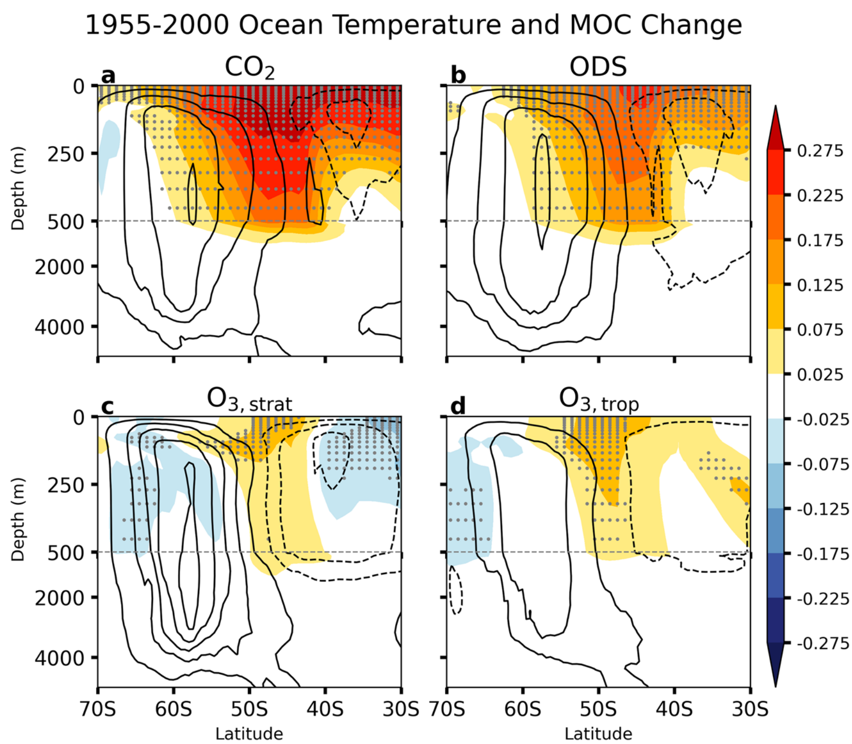

Fig. 4 | Ocean temperature and Meridional Overturning Circulation response to individual forcings. (colors) the zonal mean ocean temperature and (contours) Meridional Overturning Circulation (MOC) changes over the 1955-2000 period as a function of depth and latitude due to **a** CO_2, **b** ODSs, **c** stratospheric ozone and **d** tropospheric ozone. Dots indicate ocean temperature changes that are statistically significant at the 95% level (determined by bootstrapping). The contour interval for the MOC is 0.4 Sv, with dashed contours representing negative values.

With little surprise, Fig. 5 also shows that CO_2 is the largest contributor to Southern Ocean warming over 1955–2000, representing 57% of the net warming. More interestingly, however, and in agreement with ref. 34 (which used the same model but with a different experimental setup), we find that the tropospheric ozone contribution to Southern Ocean warming is (slightly) larger than the stratospheric ozone contribution, even though the two are not statistically different. Most importantly, and this is the third key new finding of this study, we find that both of these contributions are several times smaller than that of the radiative effects of ODSs, which represents 41% of the net warming.

Because the net warming is the residual of large warming (most notably from greenhouse gases) and cooling (most notably from aerosols) contributions, percentages expressed relative to the net warming can be misleading. For this reason, we follow S23 and further quantify the individual contributions as a fraction of total anthropogenic warming (AntW), defined here as the response to all forcings minus the cooling from

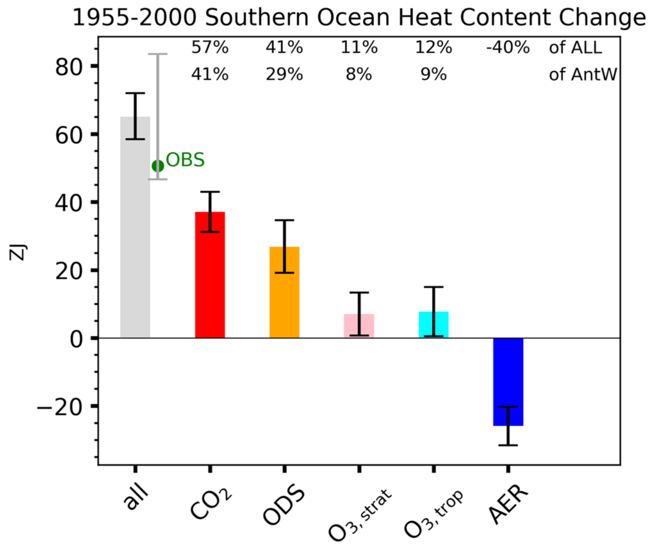

Fig. 5 | Southern Ocean heat content response to individual forcings. Southern ocean heat content change over the 1955–2000 period due to all historical forcings (ALL) and CO_2, ODSs, stratospheric ozone ($O_{3,\ strat}$), tropospheric ozone ($O_{3,\ trop}$) and aerosols (AER) separately. The black error bars represent the 5-95% confidence range in the ensemble mean (determined by bootstrapping) and the gray error bars the ±1 sigma of the ensemble spread. The numbers in the top represent the ratio between the ensemble mean response and the ensemble mean response to (top row) all forcings and (lower row) all anthropogenic warming agents (in %). The green dots denote the observed values from IAPv4[56].

anthropogenic aerosols (see Methods). This provides a clearer and more physically intuitive measure of the relative importance of the different forcings in causing ocean warming. Over the period 1955–2000, we find that anthropogenic warming agents drove an increase of 91 ZJ in SOHC. This implies that the radiative contribution of ODSs accounted for 29% of anthropogenic warming, representing a substantial fraction of the CO_2 contribution, which accounts for 41% of Southern Ocean warming. In contrast, the contributions from stratospheric ozone (8%) and tropospheric ozone (9%) are comparatively small.

Discussion

In summary, we have presented the first comprehensive quantification of the direct (radiative) and indirect (stratospheric-ozone-mediated) impacts of ODSs on historical SH climate change, focusing on the ozone depletion period from 1955 to 2000. In addition, we have contrasted those impacts with those from CO_2 and tropospheric ozone. Regarding the atmospheric circulation, we find that the radiative impacts of ODSs have played a surprisingly large role in the SH zonal wind trends, with a contribution exceeding that of CO_2, and only slightly smaller than that of stratospheric ozone depletion. In addition, ODSs appear to be more efficient than CO_2 at causing atmospheric circulation changes, which we suggest follows from the different spatial structure of the respective atmospheric temperature responses. While CO_2-induced warming is confined to the troposphere, the lower latitude warming associated with ODSs extends into the lower stratosphere, producing a broader region of enhanced meridional temperature gradients. This lower stratosphere warming from ODSs is in agreement with previous offline radiative forcing calculations[40,42] and chemistry climate model simulations[41]. However, this is the first study to report lower stratospheric tropical warming from ODS and its implications for atmosphere and ocean circulation using simulations with a comprehensive climate model.

We also find that over the 1955–2000 period, ODSs have contributed three to four times more to Southern Ocean warming than either stratospheric or tropospheric ozone. This places the previous findings that the contribution of tropospheric ozone depletion to Southern Ocean warming exceeds that of stratospheric ozone depletion[34] in the context of the direct ODS impacts. In addition, our findings resolve a long-standing confusion in previous literature regarding the role of the ozone hole in Southern Ocean warming[47,48]. While several studies have concluded that stratospheric ozone only played a minor role, one study reported that "the formation of the ozone hole" accounted for 30% of net Southern Ocean warming over the second half of the 20th century[26]. The results presented here provide strong evidence that the majority of the response reported in that study was in fact driven by the radiative effects of ODSs rather than by stratospheric ozone depletion itself. Hence, our results underscore the importance of distinguishing between the radiative impacts of ODSs and the accompanying stratospheric ozone trends in attribution studies of both past and future climate change[49].

Nonetheless, and this is the most important conclusion of our analysis, the pathway through which ODSs have affected the SH climate system is—to some degree—an academic question. What one cares about, ultimately, is the *combined* effect of ODSs on climate, and how it compares to the effect of CO_2, the preeminent agent of climate change. Assuming additivity as rough first approximation, we can here conclude that—over the second half of the 20th century—ODSs have been the main driver of atmospheric circulation trends not only summer (via ozone depletion, as is now well established) but in the annual mean as well (via radiative forcing, as seen in Fig. 1). As for ocean trends over that period, two key findings emerge from our study. First that ODSs, via the combined pathways (panels b and c in Fig. 4) are also the main driver of oceanic circulation changes, largely exceeding the impact of CO_2. Second, the combined impact of ODS on ocean heat content (37% of the anthropogenic warming) is only slightly smaller than the contribution from CO_2 (41%). These large impacts of ODSs on the climate are greatly reduced after the year 2000, as trends in the concentrations of ODSs and ozone have reversed, and are starting to cause opposite trends[37,38]. Our new findings leave little doubt as to the profound importance of the Montreal Protocol in mitigating both past and future climate change.

Methods

Model

CanESM5 is a state-of-the-art Earth System Model, which was developed at the Canadian Center for Climate Modeling and Analysis (CCCma)[35] and was used extensively to perform simulations for the sixth phase of the Coupled Model Intercomparison Project[50]. The atmospheric component, CanAM5, features 49 vertical levels, with a lid height at 1 hPa, and is run with a triangular truncation at total wavenumber 63 (T63), corresponding to an approximate resolution of 2.8° (latitude) by 2.8° (longitude).

CanESM5's ocean component, CanNEMO, is based on NEMO version 3.4.1 (ref. 51) and features 45 vertical levels with a nominal horizontal resolution of 1°. Modifications to NEMO's standard configuration include a modification of the eddy mixing length scale, which is used to compute the mesoscale eddy transfer coefficient for the Gent and McWilliams scheme[52], and the addition of a scheme that better accounts for eddy-induced diapycnal mixing observed in the deep Southern Ocean. For details on CanESM5, we refer the reader to ref. 35.

Simulations

The model simulations are an extended set of those presented in S23, to which we refer the reader for details. We use an ensemble of 20 historical simulations run with standard CMIP6 forcings, with each member run with identical forcings but with different 1850 initial conditions obtained from the preindustrial simulation at 50-year intervals. Five 20-member ensembles were branched off the standard historical simulation in the year 1955, in which we separately keep (a) CO_2, (b) ODSs, (c) stratospheric ozone, (d) tropospheric ozone, and (e) anthropogenic aerosols fixed at 1955 levels, while all other forcings follow their observed evolution. The contribution of a specific forcing is then estimated by differencing with the standard historical simulations in which all forcings follow their observed evolution. The 1955–2000 difference reported in this study is calculated as the linear trend in the resulting timeseries, multiplied by 45 years.

For Southern Ocean Heat Content, we compute the ratio of the contributions and the total anthropogenic warming. Following S23, the total anthropogenic warming (AntW) is defined as the changes due to all anthropogenic forcings minus the cooling from anthropogenic aerosols, and quantified by the 1955–2000 changes in the simulation with fixed aerosols. This approach assumes that the impact of natural forcings over the 1955–2000 period is negligible.

In our historical simulations, stratospheric and tropospheric ozone are prescribed following the CMIP6 protocols for models that lack interactive chemistry, while ODSs are prescribed uniformly in the atmosphere by time-dependent CFC-11* and CFC-12 concentrations. Following CMIP6 protocols[53], the radiative effects of all gases of lesser importance than CFC-12 are lumped together with those of CFC-11, and this is denoted CFC-11*.

Data availability

The standard CanESM5 historical simulations are available from the Earth System Grid Federation portal. All other CanESM5 simulations used in this study are available at https://crd-data-donnees-rdc.ec.gc.ca/CCCMA/publications/2026_Sigmond_Polvani.

Code availability

Analysis scripts used for this study are available at https://gitlab.com/michael.sigmond/ods_so.

Received: 24 January 2026; Accepted: 25 March 2026;
Published online: 15 April 2026

References

1. Farman, J. C., Gardiner, B. G. & Shanklin, J. D. Large losses of total ozone in Antarctica reveal seasonal ClOx/NOx interaction. *Nature* **315**, 207–210 (1985).
2. Wang, P. et al. Fingerprinting the recovery of Antarctic ozone. *Nature* **639**, 646–651 (2025).
3. Velders, G. J. M., Andersen, S. O., Daniel, J. S., Fahey, D. W. & McFarland, M. The importance of the Montreal Protocol in protecting climate. *Proc. Natl. Acad. Sci. USA* **104**, 4814–4819 (2007).
4. Ramanathan, V. Greenhouse effect due to chlorofluorocarbons: climatic implications. *Science* **190**, 50–52 (1975).
5. Gillett, N. P. et al. The Detection and Attribution Model Intercomparison Project (DAMIP v1.0) contribution to CMIP6. *Geosci. Model Dev.* **9**, 3685–3697 (2016).
6. Smith, D. M. et al. Attribution of multi-annual to decadal changes in the climate system: the Large Ensemble Single Forcing Model Intercomparison Project (LESFMIP). *Front. Clim*. **4**, https://doi.org/10.3389/fclim.2022.955414 (2022).
7. Polvani, L. M., Previdi, M., England, M. R., Chiodo, G. & Smith, K. L. Substantial twentieth-century Arctic warming caused by ozone-depleting substances. *Nat. Clim. Change* **10**, 130–133 (2020).
8. Liang, Y.-C. et al. Stronger Arctic amplification from ozone-depleting substances than from carbon dioxide. *Environ. Res. Lett.* **17**, 024010 (2022).
9. Sigmond, M. et al. Large Contribution of ozone-depleting substances to global and Arctic warming in the Late 20th century. *Geophys. Res. Lett.* **50**, e2022GL100563 (2023).
10. Bushuk, M., Polvani, L. M. & England, M. R. Comparing the impacts of ozone-depleting substances and carbon dioxide on Arctic sea ice loss. *Environ. Res. Clim.* **2**, 041001 (2023).
11. Gillett, N. P. & Thompson, D. W. J. Simulation of recent southern hemisphere climate change. *Science* **302**, 273–275 (2003).
12. McLandress, C. et al. Separating the dynamical effects of climate change and ozone depletion. Part II: Southern hemisphere troposphere. *J. Clim.* **24**, 1850–1868 (2011).
13. Polvani, L. M., Waugh, D. W., Correa, G. J. P. & Son, S.-W. Stratospheric ozone depletion: the main driver of twentieth-century atmospheric circulation changes in the Southern hemisphere. *J. Clim.* **24**, 795–812 (2011).
14. Sigmond, M., Reader, M., Fyfe, J. & Gillett, N. Drivers of past and future Southern Ocean change: stratospheric ozone versus greenhouse gas impacts. *Geophys. Res. Lett.* **38**, L12601 (2011).
15. Kang, S. M., Polvani, L. M., Fyfe, J. C. & Sigmond, M. Impact of polar ozone depletion on subtropical precipitation. *Science* **332**, 951–954 (2011).
16. Thompson, D. W. J. et al. Signatures of the Antarctic ozone hole in Southern Hemisphere surface climate change. *Nat. Geosci.* **4**, 741–749 (2011).
17. Previdi, M. & Polvani, L. M. Climate system response to stratospheric ozone depletion and recovery. *Q. J. R. Meteorol. Soc.* **140**, 2401–2419 (2014).
18. England, M. R., Polvani, L. M., Smith, K. L., Landrum, L. & Holland, M. M. Robust response of the Amundsen Sea Low to stratospheric ozone depletion. *Geophys. Res. Lett.* **43**, 8207–8213 (2016).
19. Purich, A. et al. Southern Annular Mode dynamics, projections and impacts in a changing climate. *Nat. Rev. Earth Environ.* **7**, 24–42 (2026).
20. Fogt, R. L. & Marshall, G. J. The Southern Annular Mode: variability, trends, and climate impacts across the Southern Hemisphere. *WIREs Clim. Change* **11**, e652 (2020).
21. Woollings, T., Drouard, M., O'Reilly, C. H., Sexton, D. M. H. & McSweeney, C. Trends in the atmospheric jet streams are emerging in observations and could be linked to tropical warming. *Commun. Earth Environ.* **4**, 1–8 (2023).
22. Sigmond, M., Fyfe, J. C. & Scinocca, J. F. Does the ocean impact the atmospheric response to stratospheric ozone depletion? *Geophys. Res. Lett.* **37**, 2–5 (2010).
23. Sen Gupta, A. & England, M. H. Coupled ocean–atmosphere–ice response to variations in the Southern annular mode. *J. Clim.* **19**, 4457–4486 (2006).
24. Ciasto, L. M. & Thompson, D. W. J. Observations of large-scale ocean–atmosphere interaction in the Southern Hemisphere. *J. Clim.* **21**, 1244–1259 (2008).
25. Waugh, D. W., Primeau, F., Devries, T. & Holzer, M. Recent changes in the ventilation of the southern oceans. *Science* **339**, 568–570 (2013).
26. Solomon, A., Polvani, L. M., Smith, K. L. & Abernathey, R. P. The impact of ozone depleting substances on the circulation, temperature, and salinity of the Southern Ocean: an attribution study with CESM1(WACCM). *Geophys. Res. Lett.* **42**, 5547–5555 (2015).
27. Jarníková, T., Quéré, C. L., Rumbold, S. & Jones, C. Decreasing importance of carbon-climate feedbacks in the Southern Ocean in a warming climate. *Sci. Adv.* **11**, eadr3589 (2025).
28. Menviel, L. C. et al. Enhanced Southern Ocean CO_2 outgassing as a result of stronger and poleward shifted southern hemispheric westerlies. *Biogeosciences* **20**, 4413–4431 (2023).
29. Le Quéré, C. et al. Saturation of the Southern Ocean CO_2 sink due to recent climate change. *Science* **316**, 1735–1738 (2007).
30. Lenton, A. et al. Stratospheric ozone depletion reduces ocean carbon uptake and enhances ocean acidification. *Geophys. Res. Lett.* **36**, 1–5 (2009).
31. Gille, S. T. Warming of the Southern Ocean since the 1950s. *Science* **295**, 1275–1277 (2002).
32. Cai, W. et al. Southern Ocean warming and its climatic impacts. *Sci. Bull.* **68**, 946–960 (2023).
33. Swart, N. C., Gille, S. T., Fyfe, J. C. & Gillett, N. P. Recent Southern Ocean warming and freshening driven by greenhouse gas emissions and ozone depletion. *Nat. Geosci.* **11**, 836–841 (2018).
34. Liu, W. et al. Stratospheric ozone depletion and tropospheric ozone increases drive Southern Ocean interior warming. *Nat. Clim. Chang.* **12**, 365–372 (2022).
35. Swart, N. C. et al. The Canadian Earth System Model version 5 (CanESM5.0.3). *Geosci. Model Dev.* **12**, 4823–4873 (2019).

36. Son, S.-W., Tandon, N. F., Polvani, L. M. & Waugh, D. W. Ozone hole and Southern Hemisphere climate change. *Geophys. Res. Lett.* **36**, https://doi.org/10.1029/2009GL038671 (2009).
37. Banerjee, A., Fyfe, J. C., Polvani, L. M., Waugh, D. & Chang, K.-L. A pause in Southern Hemisphere circulation trends due to the Montreal Protocol. *Nature* **579**, 544–548 (2020).
38. Zambri, B., Solomon, S., Thompson, D. W. J. & Fu, Q. Emergence of Southern Hemisphere stratospheric circulation changes in response to ozone recovery. *Nat. Geosci.* **14**, 638–644 (2021).
39. Ivanciu, I., Matthes, K., Wahl, S., Harlaß, J. & Biastoch, A. Effects of prescribed CMIP6 ozone on simulating the Southern Hemisphere atmospheric circulation response to ozone depletion. *Atmos. Chem. Phys.* **21**, 5777–5806 (2021).
40. Forster, P. M. D. F. & Joshi, M. The role of halocarbons in the climate change of the troposphere and stratosphere. *Clim. Change* **71**, 249–266 (2005).
41. McLandress, C., Shepherd, T. G., Reader, M. C., Plummer, D. A. & Shine, K. P. The climate impact of past changes in halocarbons and CO2 in the tropical UTLS region. *J. Clim.* **27**, 8646–8660 (2014).
42. Chiodo, G. & Polvani, L. M. New insights on the radiative impacts of ozone-depleting substances. *Geophys. Res. Lett.* **49**, e2021GL096783 (2022).
43. Grise, K. M. & Polvani, L. M. Understanding the time scales of the tropospheric circulation response to abrupt CO2 forcing in the southern hemisphere: seasonality and the role of the stratosphere. *J. Clim.* **30**, 8497–8515 (2017).
44. Hall, A. & Visbeck, M. Synchronous variability in the Southern Hemisphere atmosphere, sea ice, and ocean resulting from the annular mode. *J. Clim.* **15**, 3043–3057 (2002).
45. Park, S.-E., An, S.-I., Song, H., Mandal, G. & Moon, J.-Y. Inter-model diversity and its drivers in Southern Ocean meridional overturning circulation. *npj Clim. Atmos. Sci.* **8**, 380 (2025).
46. Zhu, T. & Liu, W. Evolving Southern Ocean overturning in warming climates. *Nat. Commun.* **16**, 10449 (2025).
47. Karpechko, A. Yu. et al. in *Scientific Assessment of Ozone Depletion: 2018.* Ch. 5 (World Meteorological Organization, Geneva, Switzerland, 2018).
48. Garny, H. et al. In *Scientific Assessment of Ozone Depletion: 2022.* GAW Report No. 278. 509 pp. Ch. 5 (WMO, Geneva, 2022).
49. Li, F., Newman, P. A. & Waugh, D. W. Impacts of stratospheric ozone recovery on southern ocean temperature and heat budget. *Geophys. Res. Lett.* **50**, e2023GL103951 (2023).
50. Sigmond, M. et al. Improvements in the Canadian Earth System Model (CanESM) through systematic model analysis: CanESM5.0 and CanESM5.1. *Geosci. Model Dev.* **16**, 6553–6591 (2023).
51. Madec, G. & the NEMO team. *NEMO Ocean Engine*, *Version 3.4*. (NEMO, 2012).
52. Gent, P. R. & McWilliams, J. C. Isopycnal mixing in ocean circulation models. *J. Phys. Oceanogr.* **20**, 150–155 (1990).
53. Meinshausen, M. et al. Historical greenhouse gas concentrations for climate modelling (CMIP6). *Geosci. Model Dev.* **10**, 2057–2116 (2017).
54. Hersbach, H. et al. The ERA5 global reanalysis. *Q. J. R. Meteorol. Soc.* **146**, 1999–2049 (2020).
55. Zappa, G., Pithan, F. & Shepherd, T. G. Multimodel evidence for an atmospheric circulation response to Arctic sea ice loss in the CMIP5 future projections. *Geophys. Res. Lett.* **45**, 1011–1019 (2018).
56. Cheng, L. et al. IAPv4 ocean temperature and ocean heat content gridded dataset. *Earth Syst. Sci. Data* **16**, 3517–3546 (2024).

Acknowledgements

We thank John Fyfe for initial discussions on the project, Victoria Spada for technical assistance and Nathan Gillett and Neil Swart for constructive feedback over the course of the project. The work of LMP was funded, in part, by grant #2335762 from the US National Science Foundation to Columbia University.

Author contributions

M.S. and L.M.P conceived the ideas and designed the study. M.S. performed the model simulations and the the analysis, and wrote the manuscript. L.M.P. contributed to the analysis and to the writing of the manuscript.

Competing interests

The authors declare no competing interests.

Additional information

Supplementary information The online version contains supplementary material available at https://doi.org/10.1038/s41612-026-01403-x.

Correspondence and requests for materials should be addressed to Michael Sigmond.